Numerical simulation studies of agitating paddle dependence on characteristics of the flow field in the mechanical-continuous-flow-stirred reactor for flocculation

Meng Yao[a], Zhiling Ran[a,*], Ting Chen[b], Qibao Wu[a], Xiaoqing Dong[a]

[a]*School of Traffic and Environment, Shenzhen Institute of Information Technology, Shenzhen, China, Tel. +86 15818686856; email: zhilinran_sziit@163.com (Z. Ran), Tel. +86 13662661145; email: ym808766@163.com (M. Yao), Tel. +86 13662661145; email: qibaowu_sziit@163.com (Q. Wu), Tel. +86 13480628143; email: xiaoqingdong@163.com (X. Dong)*
[b]*Guangdong GDH Water Company Limited, 518021, Shenzhen, China, Tel. +86 13267213720; email: chentinghit@163.com (T. Chen)*

ABSTRACT

The effect of stirring paddle on the flow field and particle development during the flocculation process has been investigated in a mechanical-continuous-flow-stirred reactor. Firstly, the model of different types of stirring paddles and a different combination of paddles installation height built. Then, turbulent flow fields generated under all conditions were predicted by computational fluid dynamics simulations, followed by a detailed discussion based on numerical data. The flow field velocity characteristics, turbulence characteristics, input power, cycling time and other parameters were used to evaluate the characterization of the flow field in the flocculation process. Results showed that paddle four oblique blades (α = 30°) have the shortest cycle time of water flow with the minimum input power, which provides conducive conditions for more collisions of particles and reducing the consumption of input energy. Furthermore, different installation heights of agitator paddle have a significant effect on water conditions. Results derived from the axial velocity cloud program stated paddle position set as combination 1 (H_1/H are 60, 130, 60 in respective tank cell) could provide faster flow velocity and enough particle collision, which promoted aggregation of flocs. Relatively smaller H_1/H set the former of whole reactor developed stronger turbulence to create for more vortex upward agitator blades to short cycling time. The interaction frequency between particles and paddle area was the largest and blade area is violent mixing, which is benefit of particle collision and improved flocculation effects. Based on these, appropriate paddle types and their installation height of mechanical-continuous-flow-stirred reactor should be designed to enhance particle collision and subsequent particle removal efficiency. The present study may provide meaningful insights for optimizing the design and operation of a mechanical-continuous-flow-stirred reactor for flocculation.

Keywords: Flocculation; Computational fluid dynamics (CFD); Mechanical-continuous-flow-stirred reactor; Turbulence

1. Introduction

In the water treatment process, the main role of a mechanically-agitated flocculation tank is to provide suitable hydrodynamic conditions, which results in continuous agglomeration and adherence of colloidal particles that are dispersed in water and form flocs of a large size [1,2]. The performance of this process depends upon hydrodynamics, determined by mixing intensity (which is directly related to impeller type speed and installation height for mechanical units, or feed flow for hydraulic flocculators) and geometry of flocculation unit [3–6]. The type of stirring

* Corresponding author.

paddle in the flocculation tank is the key factor in generating different hydrodynamic conditions. As for common flocculating reactors, an impeller-based mechanical stirred reactor has been widely used to accelerate destabilized particle transport and attachment for the formation of larger flocs in drinking water treatment plant [7,8]. Therefore, it is important to effectively describe the characteristic of water flow generated by the interactions between the impeller and other internals in the mechanical stirred system.

For a mechanically stirred reactor, multiple sets of experimental comparison needed to be conducted to obtain the actual process of hydraulic conditions. However, it is difficult to realize in practical flocculation treatment. Therefore, we need a standard parameter to represent the actual hydraulic conditions. The velocity gradient, G value could be used to characterize the effect of hydraulic conditions on coagulation [9,10]. The collision of particles is important for the development of flocculation. Brownian motion, speed difference of particles and flow to water are three elements to promote particle collision, especially for water flow. Theoretically, control the value of G is to control hydraulic conditions in the actual treatment. In the literature focusing on water treatment, G usually denotes the velocity gradient and its value is calculated using Camp Stein equation [11].

$$G = \left(\frac{\varepsilon_{ave}}{\upsilon}\right)^{1/2} = \left(\frac{N_p N^3 d^5}{V\upsilon}\right)^{1/2} \tag{1}$$

where G is the absolute mean velocity gradient within the computational range.

s^{-1}, is the average rate of turbulent energy dissipation, is the kinematic viscosity of water, V is the liquid volume, d is the impeller diameter, N is the rotational speed of the impeller, and N_p is the impeller power number. Traditionally, the G_{ave} is used as a global hydraulic parameter that is important for the design of flocculating reactors and the prediction/study of flocculation kinetics [11]. In our simulations, G is used to characterize the flow characteristics in the system. An empirical expression between the velocity gradient and the stable floc size has been widely used to compare floc strength within a specific experiment system [10]. The shear history effect on floc size and structural evolution has been broadly studied during kinds of mechanical stirred-tank reactors [12]. Nevertheless, a single parameter to represent flow behavior and flocculation performance was questioned by many researchers [13]. Bridgeman et al. [14], who considered that comparisons of previous flocculation-test data with new ones needed to be made cautiously since those experiments might be carried out in lab-scale flocculating reactors with different geometrical configurations. Therefore, much attention should be paid to adopt more techniques and parameters to represent flow behavior.

In the actual design process, the type and installation height of paddle in flocculation equipment is often selected based upon empirical methods, which cannot evaluate the characteristics of the flow field generated by different conditions. Due to this reason, these empirical methods cannot perform a reasonable and effective screening with regards to the type of paddle. In the flocculation process,

the inner state of water flow has a great impact on the collision and agglomeration states of particles.

However, the flow field inside the water body cannot be effectively investigated with experimental conditions [15]. Now, the computational fluid dynamics (CFD) can be adopted to perform multi-factor simulations on the relevant factors for the characteristics of the flow field in flocculation process, by predicting detailed information on spatial variation of mean velocity and turbulent fields and then, discussing their effects on cycling time and power dissipated [16,17]. Although numerous simulated studies have been conducted over several decades to investigate characteristics of turbulent flow generated in stirred tanks [18,19], very few attention to focus on the mechanical-continuous-flow-stirred reactor. Bridgeman et al. [14] have investigated the effect of reactor shape on the flow field. The jar-test simulation results exhibited that hydrodynamic environments generated by the same impeller at the same mixing speeds would be greatly different in square and cylindrical stirred tanks, which further effected flocculation behavior [20]. A comparative analysis was conducted by He et al. [21] to investigate flocculation performance in unbaffled square stirred tanks with different height-to-width ratios via experimental and CFD methods. All of these studies show that CFD technology has a deep potential to investigate particle growth dependence on the distribution of turbulent flow developed in stirred-tank flocculating reactors with different geometrical configurations [22]. As well known, the actual coagulation process is a continuous flow mechanical mixing process, since several square tanks needed to be connected in series. Unfortunately, there is little reported research focused on this aspect.

The purpose of this work was to investigate how a change in stirred paddle style and location of the impeller in the mechanical-continuous-stirred reactor would affect particle collision and aggregation in the associated turbulent flow field, by using numerical simulation methods. To more accurately evaluating characteristics of the flow field, velocity characteristics, turbulent characteristics, cycling time and power of stirring paddle were applied to represent water situation in reactors. Comparative analysis of flow field characteristics with different stirring paddle styles was conducted, then optimal paddle-style was chosen for the next step. Using the same paddle style and stirring velocity, change of flow field has been studied with different combinations of impeller installation height. All numerical simulation was applied to a commercially available CFD software, Fluent v6.3.26, to simulate the turbulent flow field within a single tank and the whole reactor, followed by a detailed discussion on numerical data. The topic has significant implications for increasing the understanding of mechanical condition on flow field characteristics, especially for the important meaning of practical engineering guiding.

2. Simulation and calculation

2.1. Establishment of the model

A continuous-flow stirred-flocculation-reactor model has been established. The water flow of this experiment was designed for 2 L/min. The whole reactor has two groups reaction pool and each group of the pool has four cells,

respective as a cell of quick mixing, quick stirring, slow mixing, and breakage. The effective size of each element was 180 mm × 180 mm × 200 mm, corresponding to a liquid volume of $V = 6.48$ L and a hydraulic retention time of 6.5 min. The diagrammatic cross-section of this reactor was shown in Fig. 1. In this simulation, G values of quick mixing, quick stirring, and slow mixing were set as 505, 66, and 23 s^{-1}.

In the present study, Ansys 14.0 was used to perform the numerical simulations for the flow field in reactor. For simplifying the calculation process, the simplified geometrical model of physical mode was established using Icem, which is the pre-processing software of CFD. The established model is shown in Fig. 2.

2.2. Grid meshing

The grid meshing process is the most important in CFD simulations, as meshing directly affects the accuracy of the simulation results. Due to the relatively complex nature of the agitation model, the calculation region within the reactor needed to be divided into various sub-regions. In this study, the multi-reference frame (MRF) was used to define the part of the paddle with a relatively complex structure as the moving region and was partitioned with a non-structured mesh and encrypted. The grid spacing of the moving region was

set to be unity since it was close to the shaft axis and had a higher rotational speed. The parts other than the paddle were defined as the stationary region and were partitioned using the structured grid, while the grid spacing was set to be 2. The data was exchanged between the moving area and the stationary area through the interface, while the grid meshing results for the reactor and paddle are shown in Fig. 3.

2.3. Numerical simulation scheme

2.3.1. Paddle type

The paddle type can affect the contact and collision of particles during the flocculation process. Therefore, three common paddle types (Fig. 4) were selected to investigate the effect of paddle type on the hydrodynamics during flocculation process.

2.3.2. Installation height of stirred-paddle

The installation height of the stirred-paddle could significantly influence the flow features in flocculation tanks. In this study, the numerical simulation of each cell of the flocculation reactor was conducted using a paddle with four oblique blades. The paddles speed of quick stirring, slow mixing and breakage cells were 180, 90, and 200 r/min,
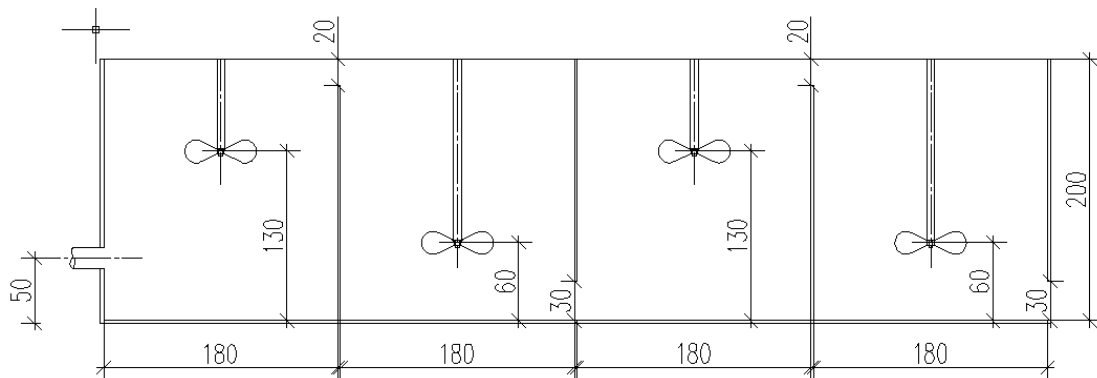

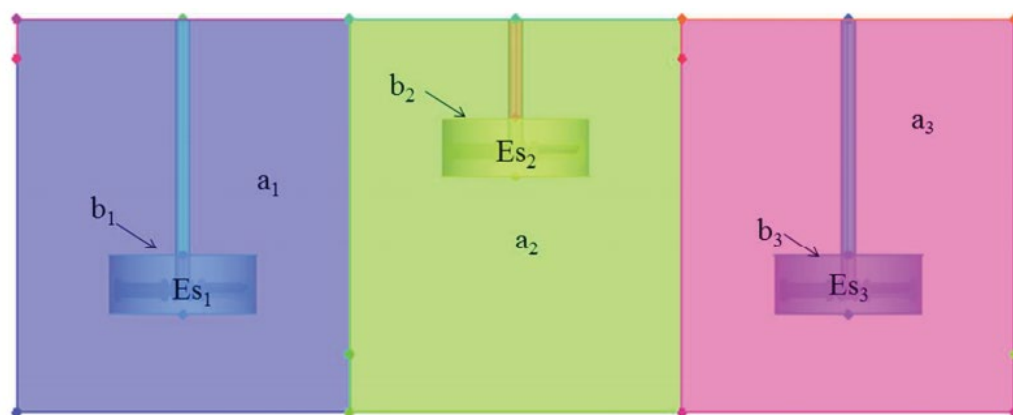Fig. 1. Schematic of the mechanically agitated flocculation tank.

Fig. 2. Geometric model of the mechanically agitated flocculation unit. (a) The moving region, (b) stator region, Es interface between the moving and stator regions.
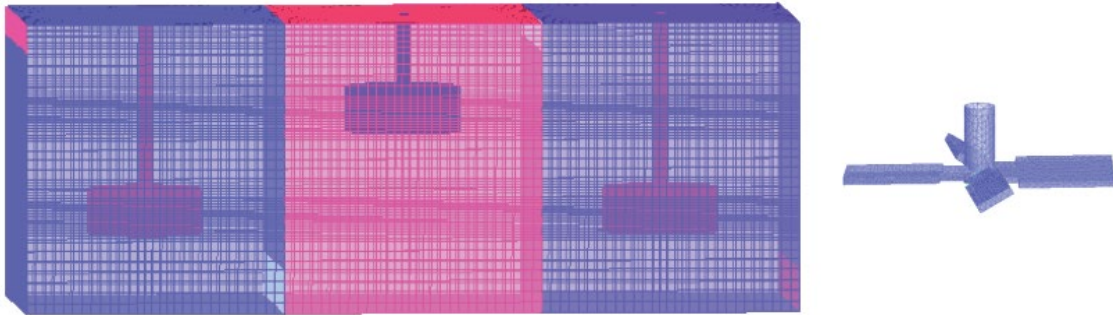
Fig. 3. Sketch of the grid meshing of mechanically agitated flocculation tank. (a) Meshing diagram of flocculation tank and (b) meshing diagram of the paddle.
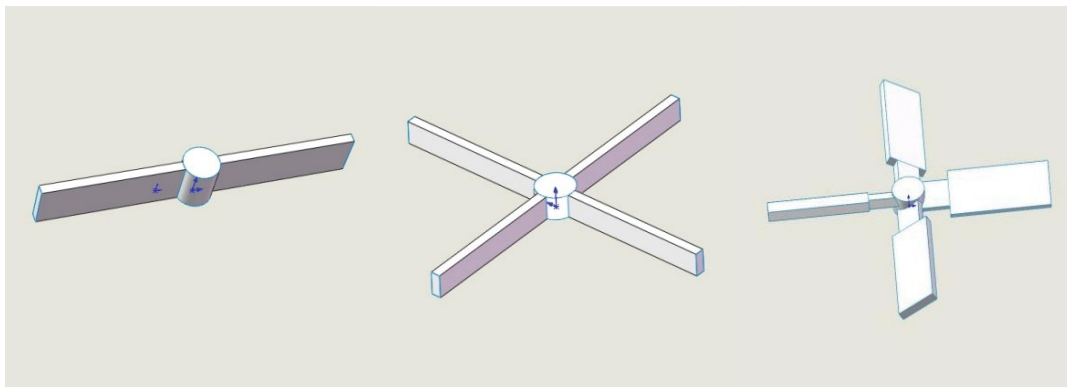

Fig. 4. Different paddle types studied in this work. (a) Long paddle with two vertical blades, (b) paddle with four vertical blades, and (c) paddle with four oblique blades (Tilt angle: $\alpha = 30°$).

respectively. The velocity contour and turbulent kinetic energy figures demonstrated the change of water flow, owing to the installation site of stirred-paddle. The ratio of H_1/H was the distance between the top of the tank and the bottom of the stirring paddle. The combination of installation height of stirred-paddles is shown in Table 1.

2.4. Numerical solution

The partitioned grid model was imported in Fluent software and the numerical solution was performed. The Fluent software was run with a three-dimensional single-precision method. Subsequently, the physical model and the grid established in Icem were imported in the solver to perform numerical solutions. The main steps followed are as follows.

2.4.1. Self-inspection of grids

The partitioned grid first performed the self-inspection in Fluent software. If the grid volume was less than 0, the grid meshing effect was considered to be poor. In this case, the grids of model again needed partitioning, since the poor partitioning can cause an error in the subsequent calculations.

2.4.2. Units within the calculation region

It was necessary to convert the default units of Fluent (m) into the default unit of Icem (cm). Additionally, the unit

Table 1
Combination of installation height of stirred-paddles

	1	2	3
	H_1/H (mm)	H_1/H (mm)	H_1/H (mm)
Cell 1	60	70	130
Cell 2	130	70	60
Cell 3	60	70	130

of angular velocity needed to be changed to revolutions per minute (rpm).

2.4.3. Selection of the solver

Fluent provides density and pressure solver. Based on density solver, coupling arithmetic was added to perform the solution of the control equation based upon the separated type of solver. Compared with the density solver, the pressure solver occupied a smaller space for the calculator and required considerably less amount of calculations. Therefore, the pressure steady solver was selected for setting the solver for the model.

2.4.4. Selection of the turbulence model

The standard k-ε model needed to solve two variables, namely the velocity and the length. The model has been

applied to calculate the engineering flow field and is considered as the simplest and more integrate dual-equation model for simulating the turbulence phenomenon. However, some deviation can occur while calculating the swirling flow and the flow with a curved wall. Therefore, for ensuring a better fitting for the turbulence with a high shear rate and a larger curvature of the flow line, a modified Random Number Generator (RNG) k-ε model was adopted in the simulation.

2.4.5. Material properties

Since the research object of the simulation was the distribution of the flow field within a mechanically agitated flocculation tank, the material system was set to be water for simplifying the simulation process.

2.4.6. Operating conditions

The component of acceleration of gravity was set along the vertical direction for simulating the effect of gravity on the flow field.

2.4.7. Boundary conditions

The inlet of the reactor was set as the velocity-inlet. The concrete hydrodynamic diameter, D, and the turbulence intensity, I, were calculated using Eqs. (2)–(4).

$$D = 4\frac{A}{\chi} \tag{2}$$

$$R_{eD} = \frac{\upsilon D}{\upsilon} \tag{3}$$

$$I = 0.16\left(R_{eD}\right)^{-1/8} \tag{4}$$

where A is the cross-sectional area of the inlet (m²), χ is the wetted perimeter, (m), υ is the initial velocity at the inlet (m/s), and ν is the kinematic viscosity (m²/s).

The pressure outlet was set as the water outlet.

The crucial step in the flow field simulation for the mechanically agitated flocculation tank was the treatment of paddle's region. The simulation adopted MRF, while the fluid within the moving region was set to rotate at the rate that was identical to that of the paddle. The bottom edges of the paddle and shaft were defined as the moving wall. The water flow within the stationary region was assumed to be stationary, while the boundary between the top part of the shaft and the stationary region was also set as the stationary boundary. The data exchange between the moving and stationary regions occurred via the interface. The boundary conditions at the free liquid surface were set as the symmetrical boundary, while other walls within the reactor were set as standard walls.

2.4.8. Controlling the solution

The difference scheme used for each variable used in the simulation is presented in Table 2.

Table 2
Difference scheme of variables used in the simulation

Variable for solving	Difference schemes selected
Pressure	Standard
Coupling between pressure and velocity	Simple
Momentum	Second-order upwind
Turbulent kinetic energy	Second-order upwind
Turbulent dissipation rate	Second-order upwind

2.4.9. Original conditions

Inlet flowrate of the mechanical flocculation tank was set as the original condition, while other parameters adopted the default values.

2.4.10. Convergent residual and measurable values

The convergent residual value was set to be 10^{-4}.

2.4.11. Beginning of the solution

The required number of iteration steps was set in the simulation. The calculations in the Fluent solver were considered as an iterative calculation procedure. The window, in which the drawing parameters varied with the number of iterations, was opened to perform the in-time monitoring of the iterative process until the iteration converged. At this point, the simulation process was completed.

2.5. Characterization of the flow field within the continuous-flow-mechanical-stirred flocculation reactor

In the simulation, the hydrodynamic software Fluent was adopted to perform visualized study on each unit of the flow field. First, characteristics inside the reactor were discussed.

2.5.1. Velocity characteristics

As for Fluent software, the visual simulation for the flow field velocity can be characterized using a cloud map and vector diagrams of the velocity. The cloud map can directly reflect the velocity of each unit area and the fluctuation intensity of each part. The turbulence with varying degrees can be characterized using different colors, which gradually transited from blue to red with the turbulence intensity changing from weak to strong, respectively. The velocity vector diagram was used to characterize the route and direction of the entire water flow. These two factors possessed important indicative significance in the characterization of the velocity.

2.5.2. Turbulent characteristics

When the particles continuously move inside water, they can form large agglomerates due to the continuous collision-adherence process. After the agglomeration, they

were separated through separating solid from a liquid. The turbulent characteristics of water flow play an important role in this process [21]. In the simulation, the RNG k-ε turbulence model with set parameters was adopted, which can characterize the degree of turbulence of flow field via turbulent energy k and turbulent dissipation rate ε and can also analyze the growth of particles under different turbulent states in a better way.

2.5.3. Cycling time

The water flowing from the bottom edge of the paddle can move along two different directions. One part of the water flow moved towards the free surface of the liquid along the reactor's wall and then moved back into the paddle's region after reaching the top. This part of the water flow was called the "upper cycle" of water flow. The other part of the water flow moved downwards to the bath's bottom along the direction of the paddle, and then, returned to the paddle's region after reaching the bottom. This part of the water flow was called the "lower cycle". The two independent cycles of the water flow formed inside the reactor are depicted in Fig. 5.

The cycling time is defined as the total time for the flow of water to finish the entire cyclic process. Its physical meaning is to represent the collision frequency between the particles inside the system and the paddle. The cycling time is calculated using Eq. (5).

$$t = \frac{\upsilon}{N_q N d^3} \tag{5}$$

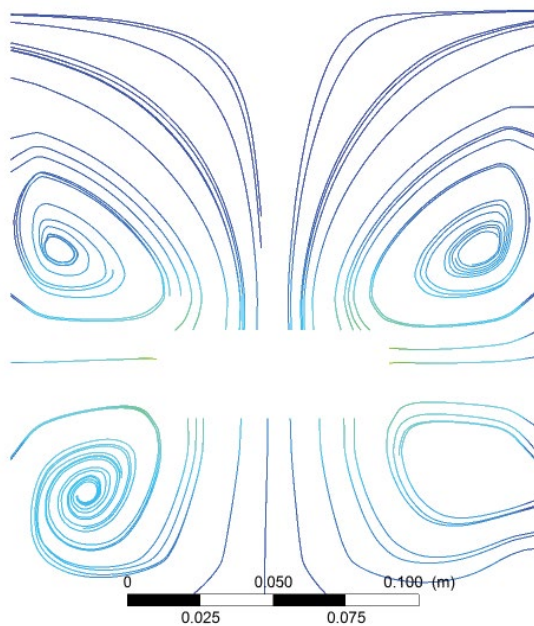where V is the volume of the reactor (mm³), N_q is the pumping capability of the paddle's blade according to the

paddle type, and d is the diameter of the paddle (mm). In the CFD simulation, the cycling time can also be calculated using Eq. (6) [23].

$$t = \frac{5.2}{N_p^{1/3} N} \left(\frac{D}{d} \right)^2 \tag{6}$$

where D is the diameter of the inscribed circle of the square reactor (mm), N is the rotational speed of paddle (rpm), and N_p is the rotation power number, calculated using Eq. (7).

$$N_p = \frac{2\pi M}{\rho N^2 d^5} \tag{7}$$

The torque of paddle, M, can be calculated using CFD, whereas the cycling time of the stirring process can be calculated using Eq. (7). As can be seen from the calculation results, the shorter cycling time indicated a more intense collision between the particles, due to which, the water flow inside the reactor generated a stronger disturbance.

2.5.4. Power of stirring paddle

In the mechanically agitated flocculation tank, the driving force for the collision and adherence between the particles resulted from the power input by the agitator. The collision frequency depended on the degree of turbulence of the reaction bath, which was determined by the input energy. The power of stirring paddle was calculated using Eq. (8).

$$P = 2\pi N M = N_p \rho N^3 d^5 \tag{8}$$

In the simulation, the input power of agitator, the velocity characteristics, the turbulence characteristics and the cycling time were used as indicators for the comprehensive evaluation of the characteristics of the flow field.

3. Results and discussion

3.1. Effect of impeller style on velocity characteristics in the flow field

A continuous-flow-mechanical-stirred flocculation reactor was adopted in the simulation. The parameters used were shown in section 2.1. The simulated height of the paddle was 70 mm (above the tank's bottom) and the paddle's rotational speed was set to be 200 rpm. For different paddle types, the simulated velocity cloud maps inside the flow field are shown in Fig. 6, in which, the left colorful strip represents the corresponding relationship between the velocity and the colors.

It can be seen from Fig. 6 that the paddle region and its surrounding areas both exhibited yellow and red colors, indicating that the velocity of this part of fluid was relatively large, and was independent of paddle type. However, the upper surface and the bottom of the flocculation tank were mostly blue, indicating that such regions had weak water flow. The small water flowrate within such areas was easy to form a dead zone in the disturbance. When the rotational

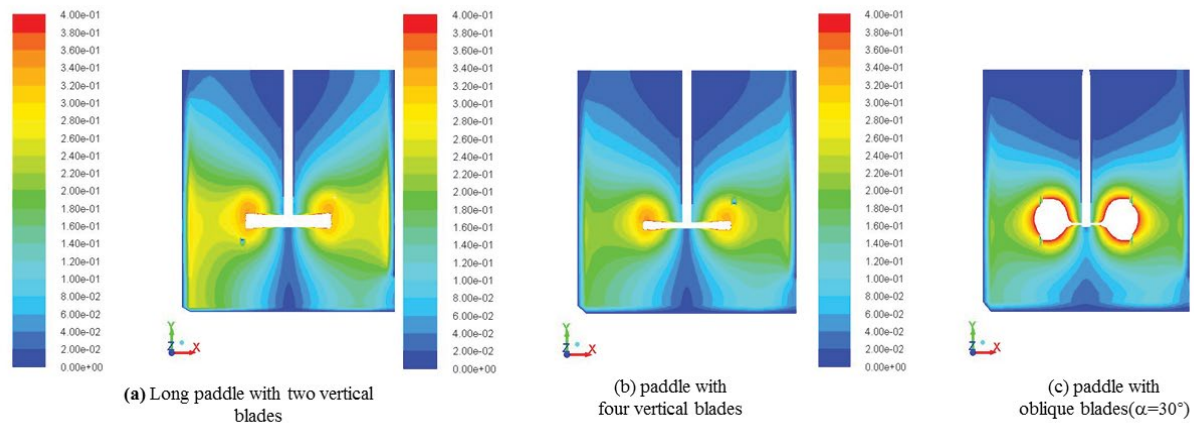Fig. 5. Streamline diagram of the mechanically agitated flocculation tank.

Fig. 6. Velocity cloud map of different paddle types.

speed of the stirring paddle remained constant, the effect of paddle type on both the fluid around the paddle and on the fluid far away from the paddle region was evident. But, it exhibited a smaller effect on the flowrate near the paddle's tip. As can be seen from Fig. 6a, when the stirring paddle-type was a long paddle with two vertical blades, its turbulence on the flow field within the entire reactor was the most evident, resulting in a uniform distribution of flow rate and the minimum dead zone. As for the flow field in the tank using the paddle with four vertical blades, its velocity distribution was poorer and is shown in Fig. 6b. The yellow area surrounding the paddle reduced, while the green area became larger, indicating that stirring surrounding the paddle was weakened. Meanwhile, the dead zones around the free liquid surface and the tank's bottom expanded. Fig. 6c shows the velocity distribution of the tank using the paddle with four oblique blades paddle (α = 30°). Its red area surrounding indicated that agitation at this position was the most intense and particles exhibited the highest collision frequency in this region. In addition, the blue area beneath the stirring blade significantly reduced, indicating that paddle effectively eliminated the "dead zone" at the bottom of the tank and improved the mixing effect at the bottom of the agitation tank. For sake as many suspended particles as possible involved in overall flow circulation and consequently to enhance the particle formation process, the dead zones, regarded as an obstacle to flow transport, must be maximally eliminated [8,24]. However, such a paddle-type exhibited a relatively weak agitation for its surrounding area and free liquid surface. Therefore, from the results of the velocity cloud diagram, the paddle with four oblique blades (α = 30°) can reak water flow co-rotation with the impeller and to increase axial flow rate, which produces a greater disturbance in the water body and thus, provides a higher probability for the particles to collide.

The velocity map provides a clearer picture of the velocity distribution in each area of the reactor. However, the map does not completely characterize the turbulence conditions of the flow field inside the entire reactor. According to the analysis of flow field characteristics presented in Section 2.5, it can be seen that the input power and the cycle time can represent the effect of different paddle types on the distribution of flow field inside the reactor more effectively.

The rotational speed of the stirring paddle in the flocculation reactor was kept constant at the value of 200 rpm. The paddle with four oblique blades (α = 30°) was set with the input power of P_0, the cycle time of t_0, and the power criterion of N_{p0}. Eqs. 6 and 7 were used to calculate the input power and the cycling time (respectively) of the flocculation tank with the other two types of the agitating paddles, as presented in Table 3. Among them, the torque M was calculated using the Fluent software.

As can be seen from Table 3, when the input power increased by 2.47–3 times, the cycling times of paddles with four vertical blades and two vertical blades did not decrease by the same numbers, and instead, decreased only by 0.69–0.74 times of the paddle with four oblique blades. The comparison between the input power and the cycling time is shown in Fig. 7, so that the relationship between the input power and cycling time can be more directly observed.

It can be seen from Fig. 7 that, when the paddle was changed from the one with two vertical blades to four oblique blades, the input power showed an evident decline. It can be seen from the comparison of cycling time that the first two agitating paddles did not exhibit the obvious reduction tendency. Therefore, based on the balancing of energy input and cycling time of water flow, the paddle with four oblique blades (α = 30°) can produce more intense disturbance under minimum input power, thus exhibiting optimum turbulent characteristics inside the flow field.

3.2. Optimization of paddle-style

For further optimizing the experimental results, the size of the paddle with two vertical blades was regulated to keep the input power and cycling time as consistent as possible. The flow field conditions generated by the paddle with two vertical blades and with four oblique blades (α = 30°) are compared and the results are presented in Table 4. Under the same conditions, the input power of the paddle with two vertical blades was 1.23 times that of the paddle with four oblique blades (α = 30°). However, the cycling time of the former was longer than that of the latter. The results indicated that paddle with two vertical blades did not generate the flow field with a better turbulence performance, except for increasing the turbulence energy loss. This result

Table 3
Comparison between the power and the cycling time of different paddle types

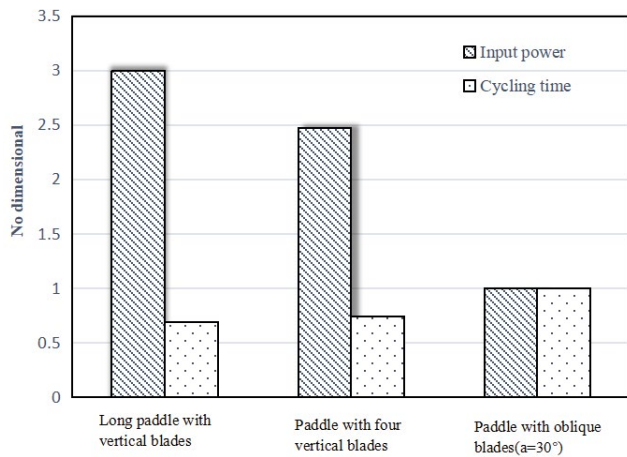| Paddle type	Torque M	Power number (N_p)	Power (P)	Cycling time (t)
Two-vertical blades	1.35	$3\,N_{p0}$	$3\,P_0$	$0.69\,t_0$
Four-vertical blades	1.11	$2.47\,N_{p0}$	$2.47\,P_0$	$0.74\,t_0$
Four oblique blades with tilt angle $\alpha = 30°$	0.45	N_{p0}	P_0	t_0

Fig. 7. Relationship between the input power and the cycling time of three paddle types.

also confirmed that the paddle with four oblique blades ($\alpha = 30°$) can effectively reduce the cycling time, increase the top-and-down exchange and disturbance in the fluid in the flocculation tank and provides better conditions for the effective collision between the particles.

After regulating the size of the paddle with two vertical blades, the flow field distributions generated by this paddle and by the paddle with four oblique blades ($\alpha = 30°$) are shown in Fig. 8. When the input power and cycling time of water flow were almost the same, the disturbance generated by a paddle with four oblique blades was much intense than that generated by a paddle with two vertical blades, exhibiting that red and yellow regions were larger. The larger red and yellow regions indicated that fluid can effectively perform exchange between the top and down parts, and can effectively enhance the collision efficiency between particles in the flocculation tank, which can promote the growth of particles and enhance the efficiency of processing unit in the flocculation process [7]. In addition, shaft's central area beneath the paddle experienced two different acting forces. One was upward entrainment generated by the paddle, while the other was downward gravitation, which weakened the flow region and flowrate. However, it can be seen

from the comparison of different paddle types that, the weak flow region generated by a paddle with four oblique blades ($\alpha = 30°$) was much lower than that generated by the square paddle with two vertical blades. The results verified that particles positioned within the areas beneath the paddle can collide with each other in a better way, and can effectively reduce the probability of flocs to precipitate at the bottom, which then forms sludge.

The inner flow field generated by paddles with four oblique blades and with four vertical blades was compared using the vector diagram of the velocity, as shown in Fig. 9. Although the paddle type was different, they can both form two moving modes, namely the "upper cycle" and the "lower cycle". The flow field generated by a paddle with four oblique blades ($\alpha = 30°$) is shown in Fig. 9a. The proportions of red and yellow areas in paddle's region were much higher than those in the region for a paddle with four vertical blades, indicating that this paddle-type exhibited a more intense disturbance than the paddle with four vertical blades [25]. The water simultaneously flowed from the bottom part of the tank and the free surface, flowed to the paddle's region along the center of the shaft and performed through agitation and mixing. The difference was, in the flow field generated by a paddle with four vertical blades and shown in Fig. 9b, the fluid exhibited a radial flow after being ejected from the rotating paddle. Then, fluid formed two independent cycles without any interaction after contacting the two sides of the flocculation tank. A flow state cannot thoroughly agitate the fluid inside the reactor, and therefore, it reduces the collision frequency between particles inside the reactor and hindered the growth of flocs, which is unfavorable for the progress of flocculation reaction. Therefore, it can be concluded that paddle with four oblique blades ($\alpha = 30°$) was conducive to form the structure of fluid more favorable for particles' collision and flocs' growth.

3.3. Effect of paddle installation height on velocity characteristics in the flow field

The installation height of paddle could significantly influence on flow field during the flocculation process. In this simulation, the installation height of the agitator paddle

Table 4
Comparison between the input power and the cycling time of different paddle types

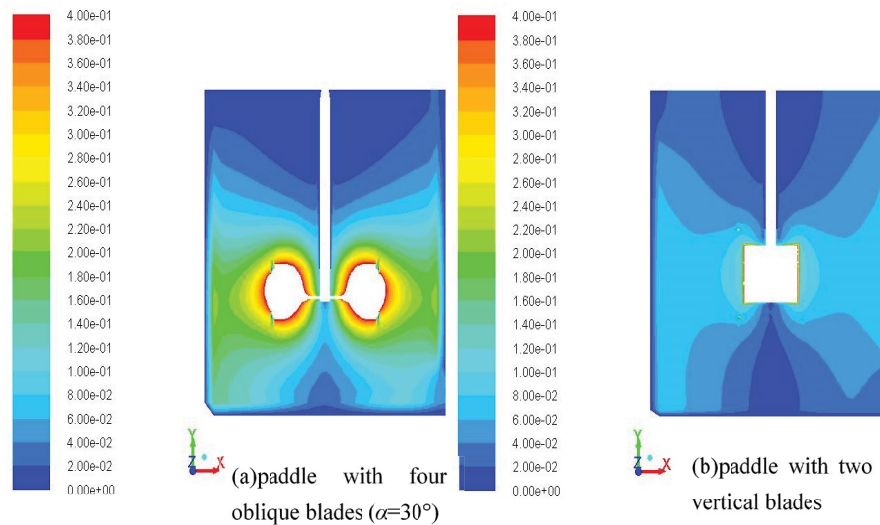| Paddle type	Torque M	Power number mm	Rotational speed rpm	Power P	Cycling time (t)
Two-vertical blades	0.554	4	200	$1.23\,P_0$	$1.12\,t_0$
Four-oblique blades	0.45	7	200	P_0	t_0

Fig. 8. Velocity cloud maps of the paddles with four oblique blades and two vertical blades. (a) Paddle with four oblique blades (α=30°) and (b) paddle with two vertical blades.

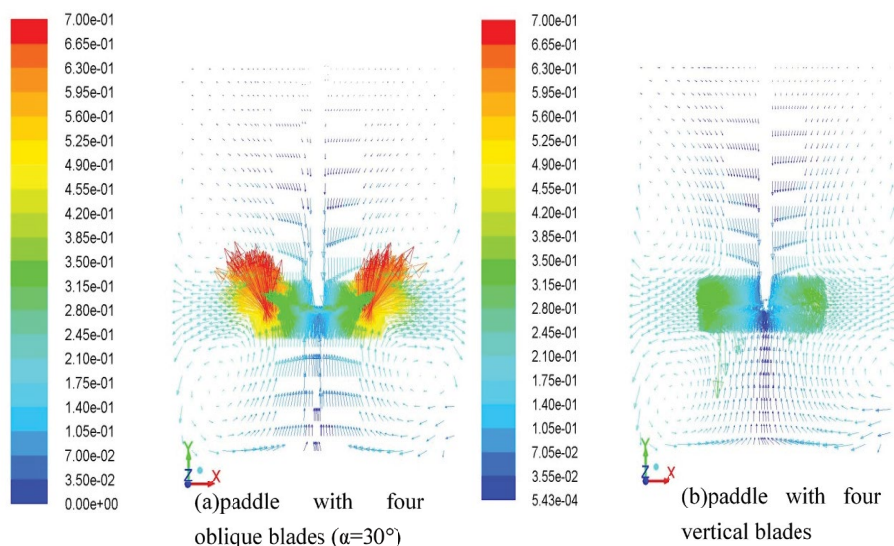Fig. 9. Velocity vector diagram of paddles with oblique blades and flat vertical blades. (a) Paddle with four oblique blades (α=30°) and (b) paddle with four vertical blades.

was changed, mainly to study whether the different position of agitating paddle in the reactor would change its influence on the surrounding fluid and intensity. The designed inlet water flowrate and the dimensions of this reactor were also set as section 3.1. The paddle's rotational speed of the three cell reaction tank were 180, 90 and 200 rpm, separately. In our study, the velocity cloud maps with a different combination of paddle installation height were applied to analysis flow field distribution. Additionally, average speed, turbulent kinetic energy, turbulent dissipation rate and cycling time were used to evaluate the performance of flow field characteristics.

Fig. 10 was shown the axial velocity cloud diagram under different combinations of paddle installation height. Apparently, see there was tight relation between flow field characterization and paddle installation height. As for the

first combination (H_1 = 60, H_2 = 130, and H_3 = 60 mm), Fig. 10a demonstrates a larger proportion area of yellow and green, while a smaller proportion of the blue area. The results stated that flow velocity is faster and the disturbance of water is more intense in the whole tank, which greatly increased the collision chance of particles. Figs. 10b and c are the second combination (H_1 = 70, H_2 = 70, and H_3 = 70 mm) and the third combination (H_1 = 130, H_2 = 60, H_3 = 130 mm), separately. Easy to see blue parts were a larger proportion than yellow and green parts. It explained the agitation is weak and fluid flow velocity is small in this reaction, which is not conducive to the aggregation of flocs.

For further information about the flow field, the average velocity (v) turbulence energy (k) and turbulence dissipation rate (ε) of each cell with different installation height
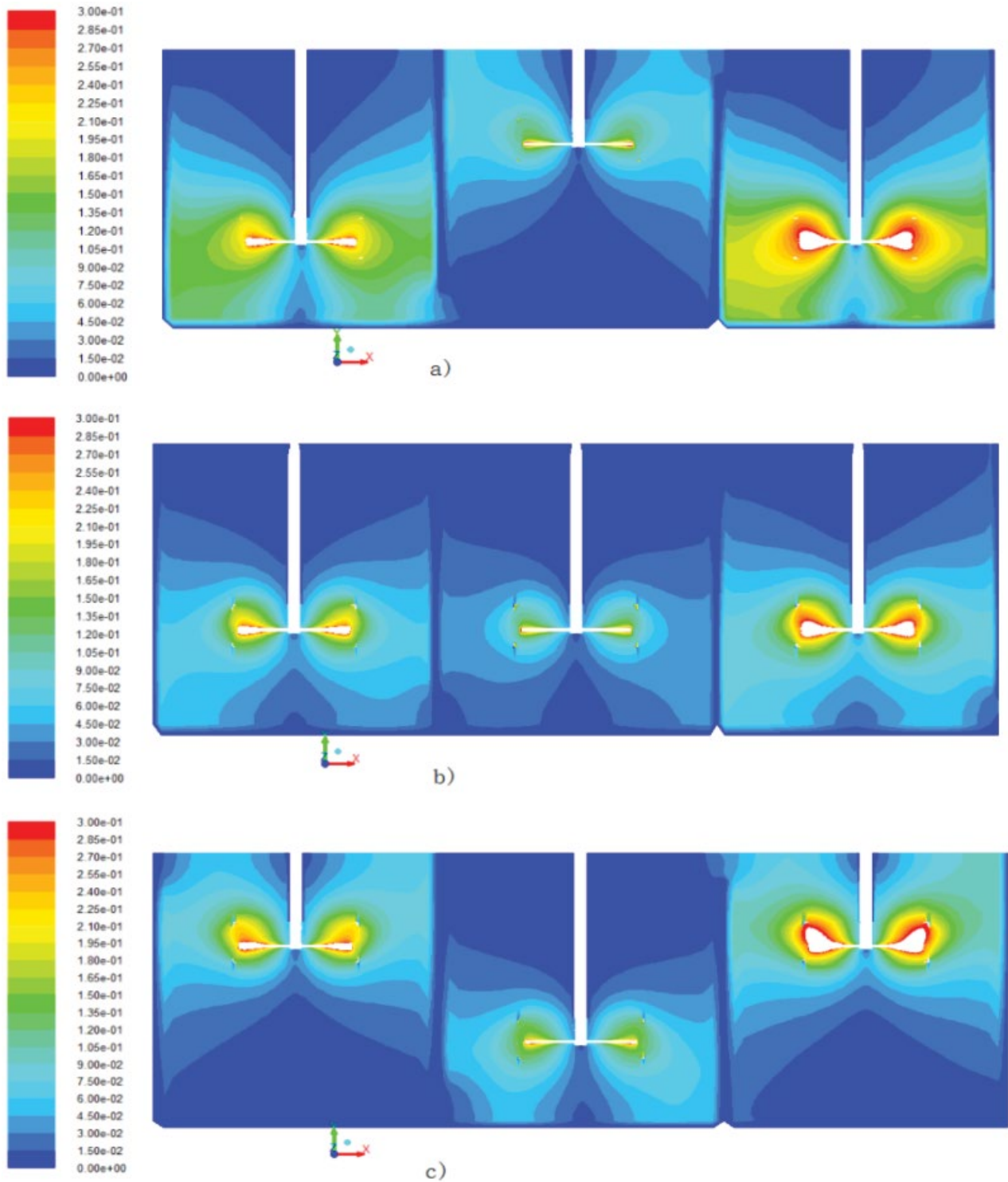
Fig. 10. Axial velocity cloud maps under different combination of paddles installation height. (a) $H_1 = 60$, $H_2 = 130$, $H_3 = 60$ mm, (b) $H_1 = 70$, $H_2 = 70$, $H_3 = 70$ mm, and (c) $H_1 = 130$, $H_2 = 60$, $H_3 = 130$ mm.

are shown in Table 5, respectively. Compared with v, k and ε from the results, it is cleared to see that combination 1 > combination 2 > combination 3. The installation height of paddle with combination 1 made the whole continuous reactor achieve the largest velocity and strongest turbulence energy. In opposite, the smallest average velocity and turbulence dissipation rate indicated the disturbance of water flow is not sufficient to prompt particle collision [25]. As for certain stirring speed, stronger turbulence developed with smaller H_1/H made for more vortex upward agitator blades.

Table 5
The average velocity of each cell with different installation height combination

	Cell 1			Cell 2			Cell 3		
	v (m/s)	k (m^2/s^2)	ε (m^2/s^2)	v (m/s)	k (m^2/s^2)	ε (m^2/s^2)	v (m/s)	k (m^2/s^2)	ε (m^2/s^2)
Combination 1	0.06473	0.2640	1.8904	0.03391	0.2118	1.7684	0.08432	0.3160	2.2333
Combination 2	0.03412	0.2113	1.6221	0.02027	0.2089	1.6160	0.04539	0.2247	1.7144
Combination 3	0.03878	0.2283	1.8420	0.02747	0.2012	1.5798	0.05224	0.2699	1.9615

More vortex promoted particle collision and adhere to each other, which further accelerate the development of flocs during the coagulation process [21]. However, turbulence areas underneath agitator blades would be restricted and resulted in the downstream of "double circulation" changing their direction before reaching the bottom, making for the appearance of "dead water zones" at bottom of the tank. Furthermore, the fluid underneath agitating blades and near the center of shaft relies on entrainment mechanisms to proceed fluid exchange [16]. Not enough water fluid circulation appeared since little farer distance between agitating blades and the bottom of the tank. The interaction frequency between particles and paddle area was largest and the blade area is violent mixing, which is benefit of particle collision and improved flocculation effects.

4. Conclusions

In the present work, CFD software was used to simulate the disturbance in the flow field, which was generated by different types of stirring paddles and a different combination of paddles installation height. The main conclusions of this study were listed as follows:

- The mechanical-continuous-flow-stirred reactor was built for the flocculation process and numerical simulation of the flow field was conducted to deeply investigate water characteristic. The flow field velocity characteristics, turbulence characteristics, input power, cycling time and other parameters were firstly used to evaluate the characterization of the flow field in the flocculation process.
- The stirring paddle-type has a significant effect on water conditions. Three different types of stirring paddles were studied and paddle having four oblique blades ($\alpha = 30°$) was found to have the shortest cycle time of water flow with the minimum input power. It shows that the type of paddle can increase the disturbance in water flow in the system, and provide conducive conditions for more collisions of particles while reducing the consumption of input energy. Furthermore, the upper and lower cycles of water flow generated in the reactor can be fully mixed and the solution at the tank's bottom and top parts can be uniformly mixed, which effectively reduces the accumulation of sludge at the reactor's bottom.
- Different installation heights of agitator paddle were changed mainly to study the effect of agitating paddle position on the surrounding fluid and intensity in the reactor. Results derived from the axial velocity cloud program stated paddle position set as combination 1 could

provide faster flow velocity and enough particle collision, which promoted aggregation of flocs. Relatively smaller H_1/H developed stronger turbulence to create for more vortex upward agitator blades, which shorted cycling time. The interaction frequency between particles and paddle area was the largest and blade area is violent mixing, which is benefit of particle collision and improved flocculation effects.

References

[1] K.Y.J. Choi, B.A. Dempsey, In-line coagulation with low-pressure membrane filtration, Water Res., 38 (2004) 4271–4281.
[2] M.A. Yukselen, J. Gregory, The reversibility of breakage, Int. J. Mineral. Process., 73 (2004) 9.
[3] D. Bouyer, C. Coufort, A. Line, Z. Do-Quang, Experimental analysis of floc size distributions in a 1-L jar under different hydrodynamics and physicochemical conditions, J. Colloid Interface Sci., 292 (2005) 413–428.
[4] M. Elazzouzi, K. Haboubi, M.S. Elyoubi, Electrocoagulation flocculation as a low-cost process for pollutants removal from urban wastewater, Chem. Eng. Res. Des., 117 (2017) 614–626.
[5] M.G. Rasteiro, I. Pinheiro, H. Ahmadloo, D. Hunkeler, F.A.P. Garcia, P. Ferreira, C. Wandrey, Correlation between flocculation and adsorption of cationic polyacrylamides on precipitated calcium carbonate, Chem. Eng. Res. Des., 95 (2015) 298–306.
[6] I.C. Tse, K. Swetland, M.L. Weber-Shirk, L.W. Lion, Fluid shear influences on the performance of hydraulic flocculation systems, Water Res., 45 (2011) 5412–5418.
[7] K. Samaras, A. Zouboulis, T. Karapantsios, M. Kostoglou, A CFD-based simulation study of a large scale flocculation tank for potable water treatment, Chem. Eng. J., 162 (2010) 208–216.
[8] F. Trivellato, On the efficiency of turbulent mixing in rotating stirrers, Chem. Eng. Process., 50 (2011) 799–809.
[9] D.C. Hopkins, J.J. Ducoste, Characterizing flocculation under heterogeneous turbulence, J. Colloid Interface Sci., 264 (2003) 184–194.
[10] P. Jarvis, B. Jefferson, J. Gregory, S.A. Parsons, A review of floc strength and breakage, Water Res., 39 (2005) 3121–3137.
[11] Y. Watanabe, Flocculation and me, Water Res., 114 (2017) 88–103.
[12] W.Z. Yu, J. Gregory, L. Campos, G.B. Li, The role of mixing conditions on floc growth, breakage and re-growth, Chem. Eng. J., 171 (2011) 425–430.

[13] C. Selomulya, R. Amal, G. Bushell, T.D. Waite, Evidence of shear rate dependence on restructuring and breakup of latex aggregates, J. Colloid Interface Sci., 236 (2001) 67–77.

[14] J. Bridgeman, B. Jefferson, S.A. Parsons, The development and application of CFD models for water treatment flocculators, Adv. Eng. Software, 41 (2010) 99–109.

[15] C. Garneau, S. Duchesne, A. St-Hilaire, Comparison of model-ling approaches to estimate trapping efficiency of sedimentation basins on peatlands used for peat extraction, Ecol. Eng., 133 (2019) 60–68.

[16] D.A. Deglon, C.J. Meyer, CFD modelling of stirred tanks: numerical considerations, Miner. Eng., 19 (2006) 1059–1068.

[17] X. Feng, J.C. Cheng, X.Y. Li, C. Yang, Z.S. Mao, Numerical simulation of turbulent flow in a baffled stirred tank with an explicit algebraic stress model, Chem. Eng. Sci., 69 (2012) 30–44.

[18] K.H. Javed, T. Mahmud, J.M. Zhu, Numerical simulation of turbulent batch mixing in a vessel agitated by a Rushton turbine, Chem. Eng. Process., 45 (2006) 99–112.

[19] M.H. Vakili, M.N. Esfahany, CFD analysis of turbulence in a baffled stirred tank, a three-compartment model, Chem. Eng. Sci., 64 (2009) 351–362.

[20] H.W. Gao, M.K. Stenstrom, Turbulence and interphase mass diffusion assumptions on the performance of secondary settling tanks, Water Environ. Res., 91 (2019) 101–110.

[21] W.P. He, L.P. Xue, B. Gorczyca, J. Nan, Z. Shi, Experimental and CFD studies of floc growth dependence on baffle width in square stirred-tank reactors for flocculation, Sep. Purif. Technol., 190 (2018) 228–242.

[22] H.W. Gao, M.K. Stenstrom, Generalizing the effects of the baffling structures on the buoyancy-induced turbulence in secondary settling tanks with eleven different geometries using CFD models, Chem. Eng. Res. Des., 143 (2019) 215–225.

[23] M. Jahoda, M. Mostek, A. Kukukova, V. Machon, CFD modelling of liquid homogenization in stirred tanks with one and two impellers using large eddy simulation, Chem. Eng. Res. Des., 85 (2007) 616–625.

[24] J. Gregory, Monitoring particle aggregation processes, Adv. Colloid Interface Sci., 147–148 (2009) 109–123.

[25] W.P. He, L.P. Xue, B. Gorczyca, J. Nan, Z. Shi, Comparative analysis on flocculation performance in unbaffled square stirred tanks with different height-to-width ratios: experimental and CFD investigations, Chem. Eng. Res. Des., 132 (2018) 518–535.